Int. J. Electrochem. Sci., 14 **(2019)** 3897 – 3915, doi: 10.20964/2019.03.51

International Journal of
ELECTROCHEMICAL
SCIENCE
www.electrochemsci.org

Corrosion Inhibition Efficiency of Cysteine-Metal ions Blends on Low Carbon Steel in Chloride-Containing Acidic Media

Abdualah Elhebshi[1], *Mohamed S. El-Deab*[2,*], *Ahmed El nemr*[3] *and Ibrahim Ashour*[1,4,*]

[1] Chemical Engineering Department, Faculty of Engineering, Elminia University, Elminia, Egypt
[2] Department of Chemistry, Faculty of Science, Cairo University, Cairo, Egypt.
[3] Environmental Division, National Institute of Oceanography and Fisheries, Kayet Bey, Elanfoushy, Alexandria, Egypt.
[4] Zewail City, University of Science and Technology, 6th October City, Giza, Egypt
[*]E-mail: msaada68@yahoo.com, iashour@zewailcity.edu.eg

Received: 11 September 2018 / *Accepted:* 18 December 2018 / *Published:* 10 March 2019

This paper addresses the effect of some metal ions (e.g., Cu^{2+}, Ni^{2+} and Fe^{2+}) in their blends with cysteine (an environmentally friendly organic compound) on the inhibition efficiency (*IE*) of the corrosion of low carbon steel (LCS) in three different media, i.e., 0.5 M H_2SO_4 in the absence and the presence of 3.5 wt% NaCl or 0.5 M Na_2SO_4. The results obtained from both electrochemical impedance spectroscopy (EIS) and electrochemical polarization measurements indicated a significant increase in *IE* of cysteine in the presence of a few micro molar amounts of Cu^{2+} ions instead of cysteine alone. On the other hand, blending cysteine with Ni^{2+} or Fe^{2+} decreased *IE*. That is *IE* reached ca. 90, 91 and 92% in the presence of 8 mM cysteine and 25 µM Cu^{2+} ions in the first, second and third medium, respectively, compared to ca. 70%, 66% and 58% in the presence of cysteine alone (i.e., in absence of Cu^{2+} ions). Moreover, polarization experiments indicated that cysteine and Cu^{2+} ions blend acts as a mixed-type inhibitor for the corrosion of LCS. The formation of Cu(I)–cysteinate complex and/or cysteine SAM at Cu atop the LCS surface (as evident from EDX and SEM results) protects the metal surface from exposure to the aggressive chloride ions. *IE* of cysteine–Cu^{2+} blend remains effectively high with time indicating its high stability in the applied chloride-containing acidic media.

Keywords: Cysteine, Low Carbon Steel, EIS, green corrosion inhibitor, acid medium**.**

1. INTRODUCTION

Alloys of carbon steel are the most commonly employed material in the construction of pipe work in the oil and gas production, such as flow lines and transmission pipelines [1–11]. However, these materials are subjected to aggressive environments in oil and gas production plants which causes rapid destruction and disintegration of the pipelines due to corrosion phenomenon. This is a major problem

related to its use in this area. For instance, internal corrosion of operating flow pipelines lead to failure disasters and safety incidents [12-14].

The use of corrosion inhibitors is a proven methodology to control corrosion problems in processes include acid solutions such as pickling processes, industrial acid cleaning, oil and gas well acidizing and for removal of rust, scale and corrosion products [15-19]. However, environmental pollution caused by various categories of inhibitors is the incentive behind the development of eco-friendly corrosion inhibitors [1-10]. In the last two decades, green corrosion inhibitors emerged as cheap, effective materials of zero or low negative environmental impact. Thus, the use of non–toxic corrosion inhibitors has also become one of the major selection requirements [20-22].

In this regard, cysteine (an organic green compound, amino acid) is a promising candidate. It was employed as a corrosion inhibitor for several metals and alloys, such as Cu [24-26], Pb–Ca–Sn ternary alloys [23], Vanadium [15], Fe and steels [16,17] as well as Cr–Co–Mo alloys [18]. The inhibition efficiency (*IE*) of cysteine against the corrosion phenomenon depends on the pH of the solution and its composition together with the nature of the metal. [24, 26-31].

Cysteine (thiol-contining compound) shows a strong tendency to chemisorb at the surface of Au, Ag, and Cu [32-34] in such a way that the accessible surface area of the metal in contact to solution decreases and thus retards its corrosion rate [35]. Moreover, cysteine is physisorbed at Fe and carbon steel surfaces and reduces its corrosion rate in acidic media [16, 36, 37].

The target in this study is to assess the inhibition efficiency (*IE*) of various cysteine-metal ions blends against the corrosion of low carbon steel (LCS) in three corrosive solutions (i.e., 0.5 M H_2SO_4 in the presence and the absence of 3.5wt% NaCL or 0.5 M Na_2SO_4) by the addition of a few (micro molar) amounts of Ni^{2+}, Fe^{2+} and Cu^{2+} ions. The results of potentiodynamic polarization and the Electrochemical Impedance Spectroscopy (EIS) are presented. Moreover, Energy Dispersive spectroscopy (EDX) and Scanning Electron Microscopy (SEM) are used to characterize the surface and the species composition at the surface of the inhibited LCS.

2. EXPERIMENTAL

2.1. Solutions and Chemicals

L-Cysteine molecule, $C_3H_7NO_2S$, (amino acid), 99% pure powder, was used as eco-friendly corrosion inhibitor. Three Corrosive media (electrolytes): (A) 0.5 M H_2SO_4, (B) 3.5wt% NaCl + 0.5 M H_2SO_4, and (C) 0.5 M Na_2SO_4 + 0.5 M H_2SO_4 were prepared by diluting concentrated sulfuric acid (98%) to a required concentration using deionized water and adding the calculated amount of the respective salt. The inhibitor stock solutions were prepared by dissolving the required amount of cysteine in the respective electrolyte. The three testing corrosive solutions containing different concentrations of cysteine (2, 4 or 8 mM of cysteine) in the absence and the presence of 25, 50 and 150 µM of Cu^{2+}, Ni^{2+} or Fe^{2+} ions.

2.2. Metal alloy, corrosion cell and Devices

A rod of LCS alloy – with the following composition (wt. %): 0.068 C, 0.249 Si, 0.662 Mn, 0.015 P, 0.022 S, 0.027 Ni, 0.031Cu, 0.122 N, 98.62 Fe– has been used as the working electrode. The electrode was sealed by Teflon coat and epoxy resin leaving a two dimensional exposed surface area of 0.64 cm^2. A graphite rod (1 cm diameter × 15 cm length) and a saturated calomel electrode (SCE) were used as the counter and the reference electrodes, respectively. The testing media were: 0.5 M H_2SO_4, 3.5 wt% NaCL + 0.5 M H_2SO_4, and 0.5 M Na_2SO_4, + 0.5 M H_2SO_4,

A conventional three-electrode glass cell was used to carry out the electrochemical measurements using a Gamry Potentiostat (model Series-G 300) controlled with Gamry Fram work version 6.12, DC105 and EIS300 software. The impedance measurements were performed at a frequency range of 100 kHz to 0.1 Hz with a peak-to-peak amplitude of 10 mV using a.c. signals under the open circuit potential (OCP) conditions of LCS. The obtained impedance spectra were analyzed using EQUIVALENT CIRCUIT software.

2.3. Experiment Methodology

At the beginning of each experiment, the working electrode was polished on wet SiC papers of successively finer grades, washed with distillated water, degreased in ultrasonic-bath with ethanol and finally dried and then immersed in the test solution. The various electrolytes were prepared using distillated water and analytical grade chemicals. All data reported in this research (current, impedance, resistance) are with respect to the geometric surface area of the working electrode (0.64 cm^2). The electrochemical measurements were conducted at room temperature (25 ± 1^oC). EIS and polarization measurements were performed after attaining a steady value of the OCP by immersing the working electrode in the test solution for at least 30 min. The polarization curves were measured potentiodynamically at a scan rate of 5 mV/s starting from the OCP towards the cathodic direction (ca. -250 mV vs. OCP) then the potential scan was reversed to a final potential of ca. +250 mV vs. OCP. Scanning electron microscopy (FEI-SEM QUANTA 250) was applied to evaluate the sample surface corrosion. The EDX (Energy dispersive spectroscopy) spectra were used to investigate elemental composition of the corroded surface.

3. RESULTS AND DISCUSSION

3.1. EIS measurements

Electrochemical Impedance spectroscopy (EIS) technique was used to study the inhibition efficiency (*IE*) of cysteine against the corrosion of LCS and the influence of adding a few micromolar amounts of Cu^{2+},Ni^{2+} or Fe^{2+} ions in three different electrolytes. Figures 1-6 display the obtained Nyquist plots recorded for LCS in the three media i.e., 0.5 M H2SO4 in the absence and the presence of 3.5 wt% NaCl or 0.5 M Na_2SO_4 in the absence and presence of 8 mM of cysteine with different concentrations of Cu^{2+} ions (Figures 1-3) cysteine with different concentrations of Ni^{2+} and Fe^{2+} ions

(Figures 4-6). The electrode was immersed at OCP for 30 min before the measurements. Figures 1-3 illustrate that the diameter of the semicircles increases (i.e., R_p increases) with the increase of cysteine concentration in the electrolyte which indicates that cysteine effectively protect the surface of LCS against corrosion. The addition of a few micromolar amounts of Cu^{2+} ions causes a further increase in the diameter of the semicircle indicating an increase in corrosion resistance of the LCS surface. This demonstrated that the presence of Cu^{2+} ions caused a significant enhancement of the inhibiting efficiency of cysteine. On the other hand, Figures 4-6 show that the diameter of the semicircles decreases with the addition of Ni^{2+} and Fe^{2+} ions to the electrolyte, in the presence of 8 mM Cysteine.

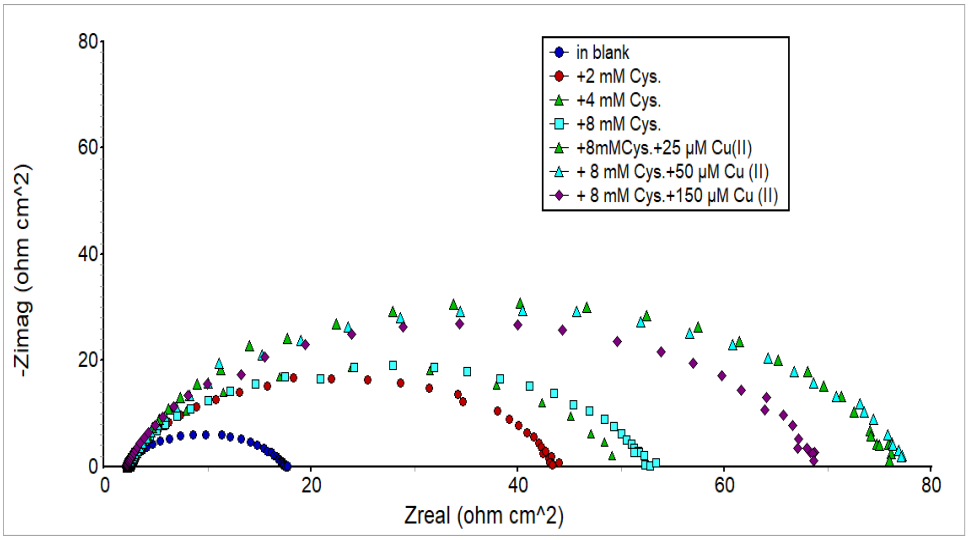

Figure 1. Nyquist plot of LCS obtained in 0.5 M H_2SO_4 containing various concentrations of cysteine and Cu^{2+} ions at 298 K.

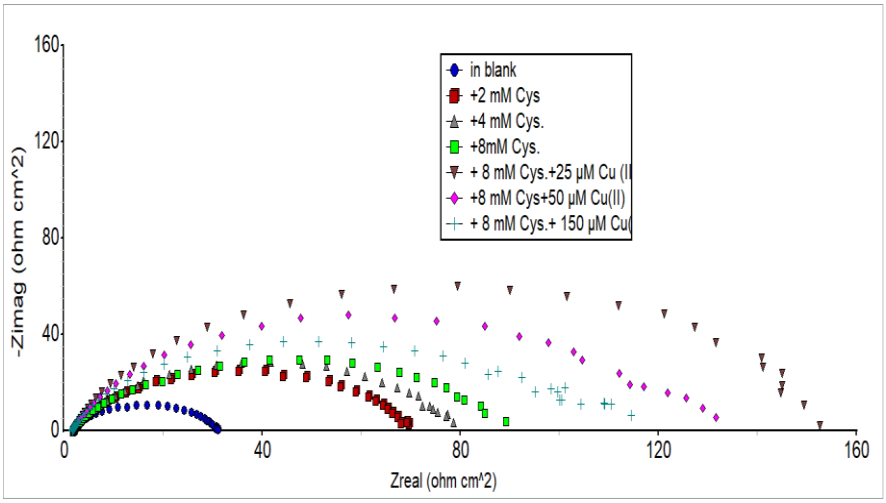

Figure 2. Nyquist plot of LCS recorded in 3.5 wt% NaCl + 0.5 M H_2SO_4 solution containing various concentrations of cysteine and Cu^{2+} ions in at 298 K.

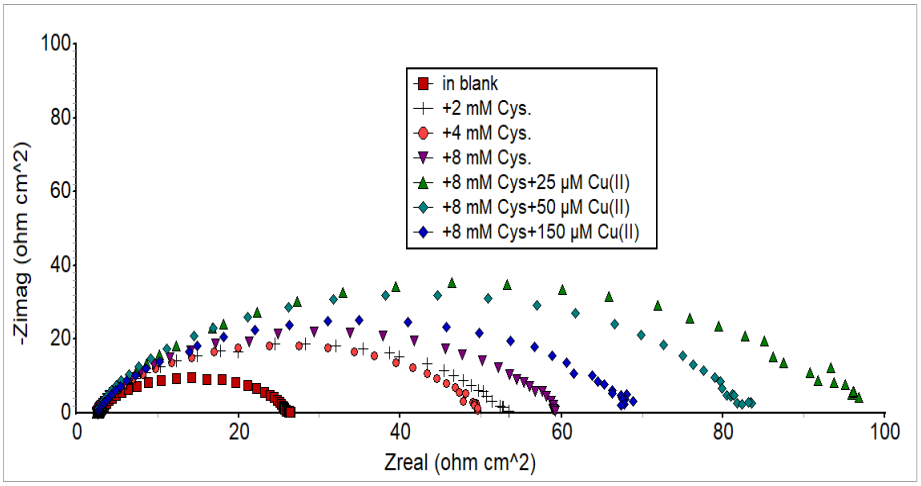

Figure 3. Nyquist plot of LCS recorded in 0.5 M Na_2SO_4 + 0.5 M H_2SO_4 solution containing various concentrations of cysteine and Cu^{2+} ions in at 298 K.

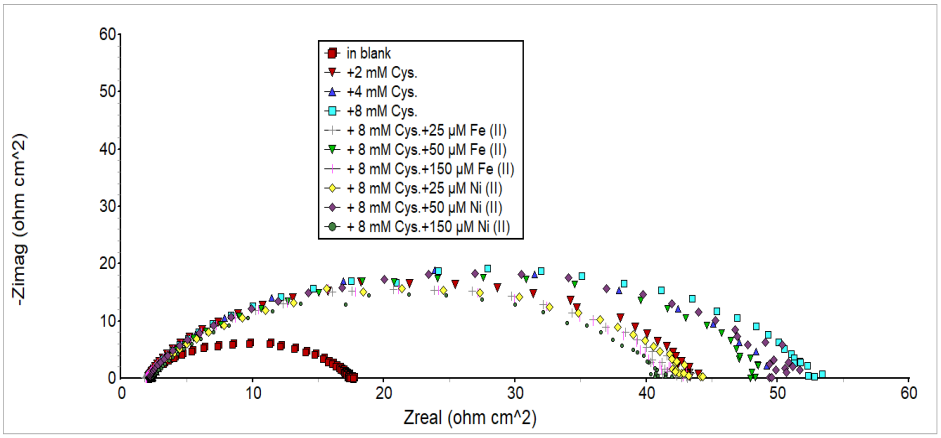

Figure 4. Nyquist plot of LCS recorded in 0.5 M H_2SO_4 solution containing various concentrations of cysteine and Ni^{2+} or Fe^{2+} ions at 298 K.

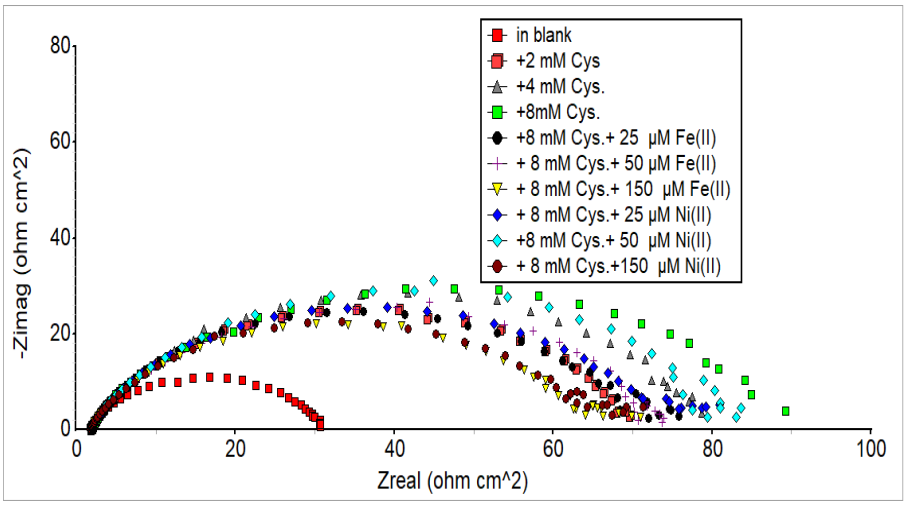

Figure 5. Nyquist plot of LCS recorded in 3.5 wt% NaCl + 0.5 M H_2SO_4 solution containing various concentrations of cysteine and Ni^{2+} or Fe^{2+} ions at 298 K.

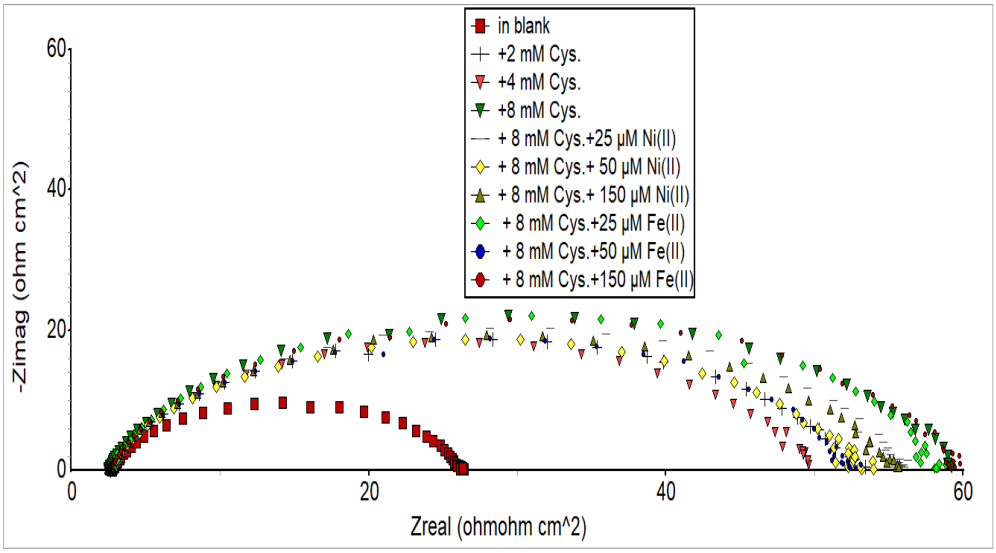

Figure 6. Nyquist plot of LCS recorded in 0.5 M Na_2SO_4 + 0.5 M H_2SO_4 solution containing various concentrations of cysteine and Ni^{2+} or Fe^{2+} ions at 298 K.

An electrical equivalent circuit represented in Fig. 7 was used to simulate the EIS data and to determine the equivalent resistances, then the related efficiencies. The equivalent circuit consists of a parallel combination of a resistor, R_p, representing the polarization resistance and a capacitor, C_{dl}, represents the double layer capacity of the electrode/electrolyte interface, in a series with the solution resistance component (R_s). The relation between the impedance of applied circuit, Z, and the frequency of the a.c. signal (f), R_p, R_s, and CPE_{dl}, is presented in equation (1) [38]:

$$Z = R_s + \left(\frac{R_p}{1 + (j2\pi f C_{dl} R_p)^{\alpha}} \right) \quad (1)$$

where α is an empirical parameter ($0 \leq \alpha \leq 1$) which indicates the extent of deviation from the ideal RC-behavior of the electrode/electrolyte interface. The surface of the LCS turns rough due to its corrosion in the acidic medium, thus, the capacitance is presented through a constant phase element (CPE). Tables 1-3 list the calculated parameters of the equivalent circuit in the three investigated media at various concentrations of cysteine in the absence and the presence of a few micromolar amounts of Cu^{2+} ions. Inhibition efficiency was then calculated using equation (2) [33-35, 39, 40].

$$IE\% = \left(1 - \left[\frac{R_p^{(blank)}}{R_p^{(inh.)}} \right]\right) \times 100 \quad (2)$$

Where $R_p^{(blank)}$ and $R_p^{(inh.)}$ are the polarization resistances in the absence and the presence of the inhibitor, respectively.

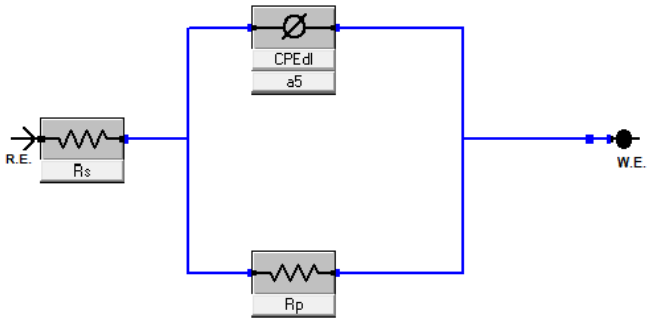

Figure 7. Schematic representation of the proposed equivalent circuit. Rs, Rp and CPE represent solution resistance, polarization resistance and the capacitance of interface double-layer respectively.

Table 1. Fitting parameters of the proposed equivalent circuit and calculated inhibition efficiency (*IE*) of LCS in 0.5 M H_2SO_4 containing various concentrations of cysteine and different concentration of Cu^{2+} ions. Data collected from EIS measurements.

Electrolyte composition	Rp ($\Omega\ cm^2$)	CPE×10^6($\Omega^{-1}cm^{-2}S^{\alpha}$)	α	*IE* %
0.5 M H_2SO_4 (A)	15.25	372	0.863	-
A + 2 mM Cysteine	41.57	224	0.853	63.31
A + 4 mM Cysteine	47.49	209	0.845	67.88
A + 8 mM Cysteine (A1)	50.14	225	0.836	69.58
A1 + 25 µM Cu^{2+}	74.68	233	0.88	79.58
A1 + 50 µM Cu^{2+}	75.39	330	0.844	79.00
A1 + 150 µM Cu^{2+}	67.05	304	0.859	77.26

Table 2. Fitting parameters of the proposed equivalent circuit and calculated inhibition efficiency (*IE*) of LCS in 3.5 wt% NaCl + 0.5 M H_2SO_4 containing various concentrations of cysteine and different concentration of Cu^{2+} ions. Data collected from EIS measurements.

Electrolyte composition	Rp ($\Omega\ cm^2$)	CPE×10^6($\Omega^{-1}cm^{-2}S^{\alpha}$)	α	IE %
0.5 M H_2SO_4 +3.5%NaCl (B)	28.75	399	0.858	-
B + 2 mM Cysteine	68.44	306	0.804	57.9
B + 4 mM Cysteine	77.75	315	0.801	63.1
B + 8 mM Cysteine (B1)	84.95	331	0.785	66.2
B1 + 25 µM Cu(II)	151.9	234	0.85	81.1
B1 + 50 µM Cu(II)	136.07	287	0.84	78.9
B1 + 150 µM Cu(II)	117.45	372	0.849	75.5

Table 3. Fitting parameters of the proposed equivalent circuit and calculated inhibition efficiency (*IE*) of LCS in 3.5 wt% NaCl + 0.5 M H_2SO_4 containing various concentrations of cysteine and different concentration of Cu^{2+} ions. Data collected from EIS measurements.

Electrolyte composition	Rp (Ωcm^2)	CPE×10^6($\Omega^{-1}cm^{-2}S^{\alpha}$)	α	*IE* %
0.5 M H_2SO_4 +0.5 M Na_2SO_4 (C)	23.46	246	0.858	-
C + 2 mM Cysteine	49.35	219	0.868	52.5
C + 4 mM Cysteine	47.09	227	0.843	50.2
C + 8 mM Cysteine (C1)	56.51	214	0.846	58.5
C1 + 25 µM Cu^{2+}	93.34	314	0.824	74.9
C1 + 50 µM Cu^{2+}	80.19	277	0.857	70.7
C1 + 150 µM Cu^{2+}	65.70	393	0.831	64.3

Inspecting Tables 1-3 demonstrates a significant enhancement of *IE* of cysteine in the presence of Cu^{2+} ions. *IE* values were recorded for 8 mM cysteine (without Cu^{2+} ions) as 69.6, 66.2, and 58.5%, in 0.5 M H_2SO_4 solution in the absence and the presence of 3.5 wt% NaCL and 0.5 M Na_2SO_4, respectively. The addition of 25 µM Cu^{2+} ions showed a pronounced increase of *IE* in the three media upto 79.6, 81.1 and 74.7%, respectively. Whereas, further increase of Cu^{2+} ions concentration leads to adverse effect, i.e., decrease of *IE*. This can be reasonably explained in view of the deposition of metallic Cu atop the surface of LCS and thus promotes the hydrogen evolution reaction (HER) and consequently increase the overall rate of corrosion of LCS.

3.2. Potintiodynamic and Weight- loss measurements

To further confirm the EIS data, potentio-dynamic measurements were conducted. Figure 5 illustrates an example of potintiodynamic curves recorded for LCS in 0.5 M H_2SO_4 containing various concentrations of cysteine without/with different amounts of Cu^{2+} ions concentrations in the electrolyte in which the anodic branch represents the dissolution of LCS, while the cathodic branch represents the HER. Figures 8-10 demonstrate that in the addition of cysteine-Cu^{2+} ions blends caused a marked decrease of the cathodic as well as the anodic current densities. This indicates that the blend acts as a mixed-type corrosion inhibitor. Tables 4-6 list the corresponding corrosion current densities ($I_{corr.}$) (as estimated by extrapolation of the anodic and cathodic curves to the corresponding OCP). The corresponding *IE* values were calculated using Equation (3) [38].

Inspection of these tables reveals that cysteine-Cu^{2+} ions caused a pronounced inhibitive effect, proving the enhancement effect of copper ions on cysteine inhibition against low carbon steel corrosion, consistently with the conclusions of Tables 1-3.

$$IE\% = (1 - [\frac{I_{corr.inh}}{I_{corr.blank}}]) \times 100 \quad (3)$$

Where $I_{corr.inh}$ and $I_{corr.blank}$ represent the corrosion currents of LCS (at OCP) in the inhibited and the uninhibited solutions, respectively. *IE* values of 80.1, 78.7, and 74.4% were obtained in the presence of 8 mM of cysteine with 25 µM of Cu^{2+} ions, in 0.5 M H_2SO_4, 3.5 wt% NaCl + 0.5 M H_2SO_4, and 0.5 M Na_2SO_4 + 0.5 M H_2SO_4, respectively which is consistent with the values calculated on the basis of the EIS data.

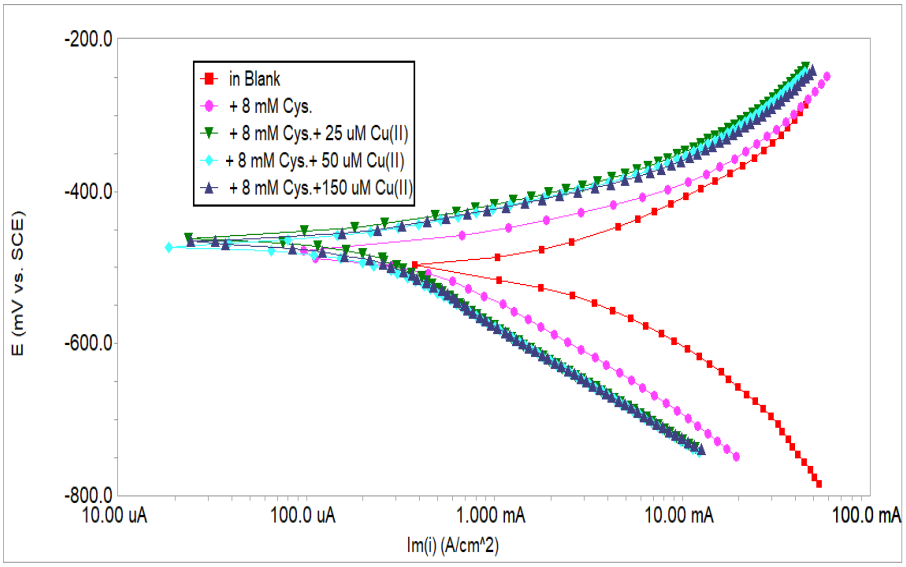

Figure 8. Polarization curves of LCS in 0.5 M H_2SO_4 containing 8 mM cysteine and various concentrations of Cu^{2+} ions. Potential scan rate: 5 mV/s.

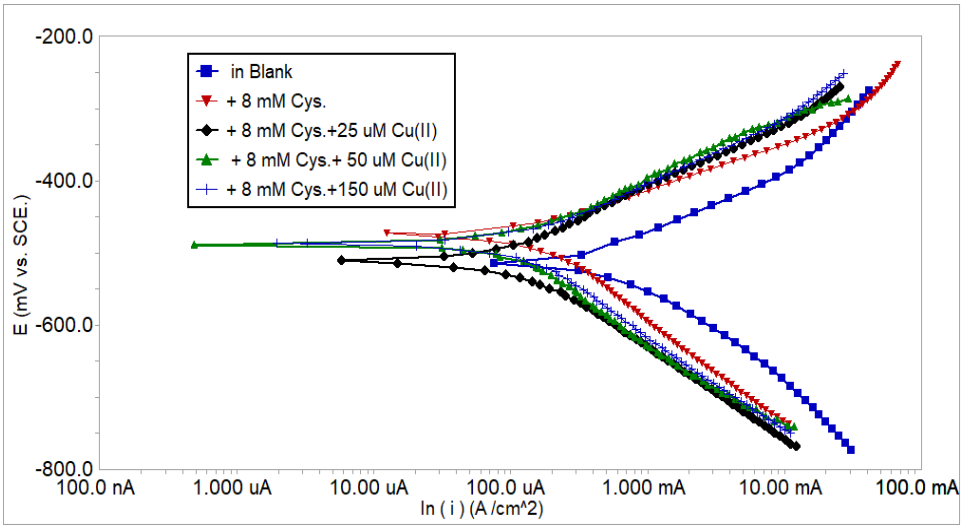

Figure 9. Polarization curves of LCS in 3.5 wt% NaCl + 0.5 M H_2SO_4 solution containing 8 mM cysteine and various concentrations of Cu^{2+} ions. Potential scan rate: 5 mV/s.

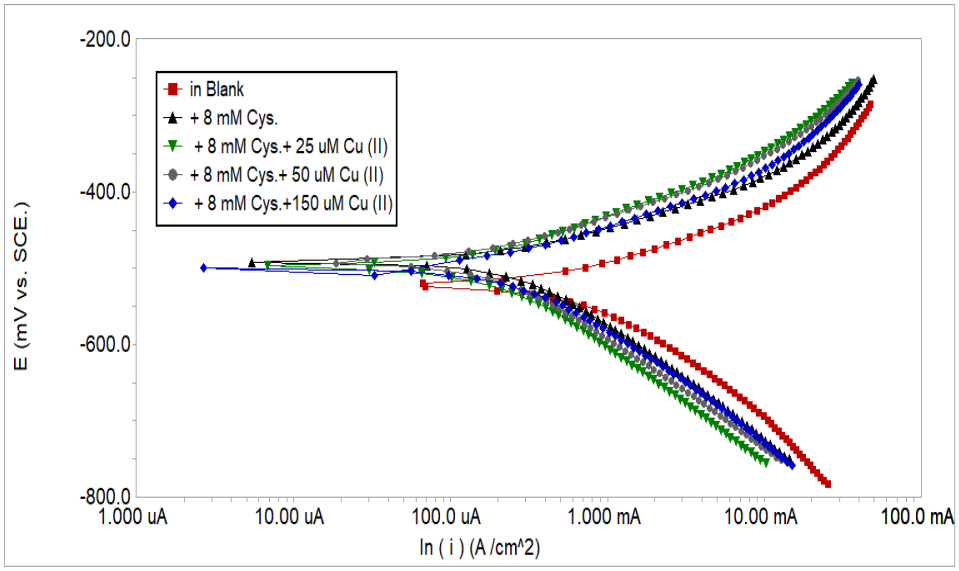

Figure 10. Polarization curves of LCS in 0.5 M Na_2SO_4 + 0.5 M H_2SO_4 solution containing 8 mM cysteine and various concentrations of Cu^{2+} ions. Potential scan rate: 5 mV/s.

Table 4. Corrosion current densities ($I_{corr.}$), anodic and cathodic Tafel slopes (β_a and β_c , respectively), corrosion potential ($E_{corr.}$) and *IE* of LCS in 0.5 M H_2SO_4 solution containing various concentrations of cysteine and Cu^{2+} ions.

Electrolyte composition	-$E_{corr.}$ (mV)	Corrosion current density ($I_{corr.}$) (mA)	βa (mV.dec^{-1})	-βc (mV.dec^{-1})	*IE* (%)
0.5 M H_2SO_4 (A)	514	0.91	98	116	-
A + 2 mM Cysteine	492	0.385	62	148	57.7
A + 4 mM Cysteine	484	0.287	62	127	68.5
A + 8 mM Cysteine (A1)	491	0.276	61	121	69.7
A1+ 25 µM Cu(II)	462	0.182	56	134	80.1
A1+ 50 µM Cu(II)	471	0. 201	66	147	77.9
A1+ 150 µM Cu(II)	467	0.193	57	132	78.8

Table 5. Corrosion current densities ($I_{corr.}$), anodic and cathodic Tafel slopes (β_a and β_c , respectively), corrosion potential ($E_{corr.}$) and *IE* of LCS in 3.5 wt% NaCl + 0.5 M H_2SO_4 solution containing various concentrations of cysteine and Cu^{2+} ions.

Electrolyte composition	-$E_{corr.}$ (mV)	Corrosion current density (I_{corr})(mA)	βa (mV.dec^{-1})	-βc (mV.dec^{-1})	*IE* (%)
0.5 M H_2SO_4 + 3.5 wt.% NaCl (B)	517	0.545	103	109	-
B + 2 mM Cysteine	497	0.205	77	137	62.4

B + 4 mM Cysteine	495	0.171	77	126	68.6
B + 8 mM Cysteine (B1)	496	0.157	90	124	71.2
B1 + 25 µM Cu^{2+}	511	0.116	120	107	78.7
B1 + 50 µM Cu^{2+}	487	0.130	97	135	76.2
B1 + 150 µM Cu^{2+}	487	0.149	91	146	72.7

Table 6. Corrosion current densities ($I_{corr.}$), anodic and cathodic Tafel slopes (β_a and β_c , respectively), corrosion potential ($E_{corr.}$) and *IE* of LCS in 0.5 M Na_2SO_4 + 0.5 M H_2SO_4 solution containing various concentrations of cysteine and Cu^{2+} ions.

Electrolyte composition	$-E_{corr.}$ (mV)	Corrosion current density (I_{corr})(mA)	βa (mV.dec^{-1})	-βc (mV.dec^{-1})	*IE* (%)
0.5 M H_2SO_4 +0.5 M Na_2SO_4 (C)	521	0.579	80	126	-
C + 2 mM Cysteine	501	0.248	59	115	57.2
C + 4 mM Cysteine	498	0.27	65	122	53.4
C + 8 mM Cysteine (C1)	491	0.236	65	128	59.2
C1+ 25 µM Cu^{2+}	498	0.154	80	117	73.4
C1+ 50 µM Cu^{2+}	492	0.173	75	123	70.1
C1+ 150 µM Cu^{2+}	499	0.207	75	114	64.2

The enhancing effect of Cu^{2+} ions on *IE* of cysteine against the corrosion of LCS is also evident from the results of the weight loss measurements which were carried out in the three media in the absence and presence of 8 mM of cysteine without/with 25 µM of Cu^{2+} ions.

Table 7 reports the values of corrosion rate (*CR*) and the corresponding *IE* values. The corrosion rate (CR, millimeters per year) was calculated from the equation (4) [41]:

$$CR == \frac{K\,W}{\mathrm{t\,A\,\rho}} \qquad (4)$$

Where *W* is the weight loss (g), *t* is the immersion time (hr), *A* is the surface area of the electrode (cm^2), ρ is the density of LCS (g cm^{-3}), and $K = 8.76 \times 10^4$ is the conversion constant that applied to express *CR* in millimeters per year when *t, A, W* and ρ values are expressed in the quoted units. IE is calculated using Equation (5) [42, 43]:

$$IE\% = (1- [W_i / W_o]) \times 100 \qquad (5)$$

where W_o and W_i is the weight loss (g) of the tested low carbon steel metal in the absence and presence of the inhibitor at a specified concentration (*i*), respectively.

Inspection of Table 7 reveals a significant reduction in *CR* with *IE* of 75, 70, and 65% in presence of 8 mM cysteine in the three media, respectively. Interestingly and consistently, with polarization and EIS data, *IE* increases up to 82, 88, and 82% in the presence of 8 mM cysteine together with 25 µM of Cu^{2+} ions in the three media, respectively.

Table 7. Weight loss, corrosion rate and *IE* data obtained from weight-loss measurements of carbon steel immersed 21 hr in three media: (A) 0.5 M H_2SO_4, (B) 3.5 wt.% NaCl + 0.5 M H_2SO_4, (C) 0.5 M Na_2SO_4 + 0.5 M H_2SO_4 in presence of 8 mM cysteine with and without 25 µM Cu^{2+} ions.

Electrolyte	Inhibitor concentration	*Wi* (g)	*CR*(mm/y)	*IE%*
0.5 M H_2SO_4 A	-	(*Wo* =0.065)	34.65	-
	A+ 8 mM Cys.(A1)	0.017	8.7	75
	(A1) + 25 µM Cu^{2+} ions	0.012	6.4	82
3.5 wt.% NaCl + 0.5 M H_2SO_4 B	-	(*Wo* = 0.016)	8.7	-
	B + 8 mM Cys.(B1)	0.005	2.6	70
	B1 + 25 µM Cu^{2+} ions	0.002	1	88
0.5 M Na_2SO_4 + 0.5 M H_2SO_4 C	-	(*Wo* = 0.065)	34.3	-
	C + 8 mM Cys.(C1)	0.022	11.9	65
	C1 + 25 µM Cu^{2+} ions	0.011	6	82

3.4. Stability of Cu(II)–cysteine inhibitor blend in the three media

EIS experiments were conducted in the presence of 8 mM of cysteine and 25 µM of Cu^{2+} ions in the three testing corrosive media (A, B and C) at various time intervals to assess its long-term stability. The results are shown in Tables 8-10 and Figures 11-13.

The data in Tables 7-9 and Fig. 8-10 show that during the first hour of immersing of LCS in the three corrosive electrolytes, the inhibitor blend reached a maximum inhibition efficiency of 89.7%, 91.1%, and 91.5% respectively in the three media. The corrosion inhibition efficiency remains effectively unchanged at this high value for a prolonged immersion time of about 6 hours. This indicates a good stability of the cysteine- copper ions inhibitor blend in the three testing corrosive media. The long-lasting time of corrosion inhibition efficiency of cysteine- Cu^{2+} ions blend can also be proved by the results of weight loss experiments. Weight loss results showed that during 21 hours of immersion time of the LCS samples in the three media in the present of 8 mM cysteine + 25 µM of Cu^{2+} ions, the *IE* increases and remains at ca. 82, 88, and 82% respectively.

Table 8. Variation of R_p and *IE* with immersion time of LCS in 0.5 M H_2SO_4 solution containing 8 mM cysteine + 25 µM Cu^{2+} ions.

Testing time /min	Blank solution (0.5 M H_2SO_4)	0.5 M H_2SO_4+ 8 mM Cys.+ 25 µM Cu^{2+} ions	*IE*%
	R_p (ohm)	R_p (ohm)	
30	15.25	74.68	79.6
60	13.6	75.16	81.9
120	11.05	64.69	82.9
240	7.31	55.97	86.9
360	5.25	50.92	89.7

Table 9. Variation of R_p and *IE* with immersion time of LCS in 3.5 wt% NaCl + 0.5 M H_2SO_4 solution containing 8 mM cysteine + 25 µM Cu^{2+} ions.

Testing time /min	Blank solution (3.5 wt% NaCl+ 0.5 M H_2SO_4)	3.5 wt% NaCl+ 0.5 H_2SO_4 + 8 mM Cys.+ 25 µM Cu^{2+} ions.	*IE%*
	Rp (ohm)	Rp (ohm)	
30	28.75	151.9	81.1
60	22.89	145.0	84.2
120	17.11	142.8	88.1
240	14.12	140.2	89.9
360	12.25	137.0	91.1

Table 10. Variation of R_p and *IE* with immersion time of LCS in 0.5 M Na_2SO_4 + 0.5 M H_2SO_4 solution containing 8 mM cysteine + 25 µM Cu^{2+} ions.

Testing time / min	Blank solution (0.5 M Na_2SO_4 + 0.5 M H_2SO_4)	0.5 M Na_2SO_4 + 0.5 M H_2SO_4 + 8 mM Cys.+25 µM Cu^{2+} ions	*IE*%
	Rp (ohm)	Rp (ohm)	
30	23.5	93.3	74.9
60	14.5	118.2	87.3
120	11.4	112.4	89.8
240	8.1	93.5	91.3
360	7.0	83.0	91.5

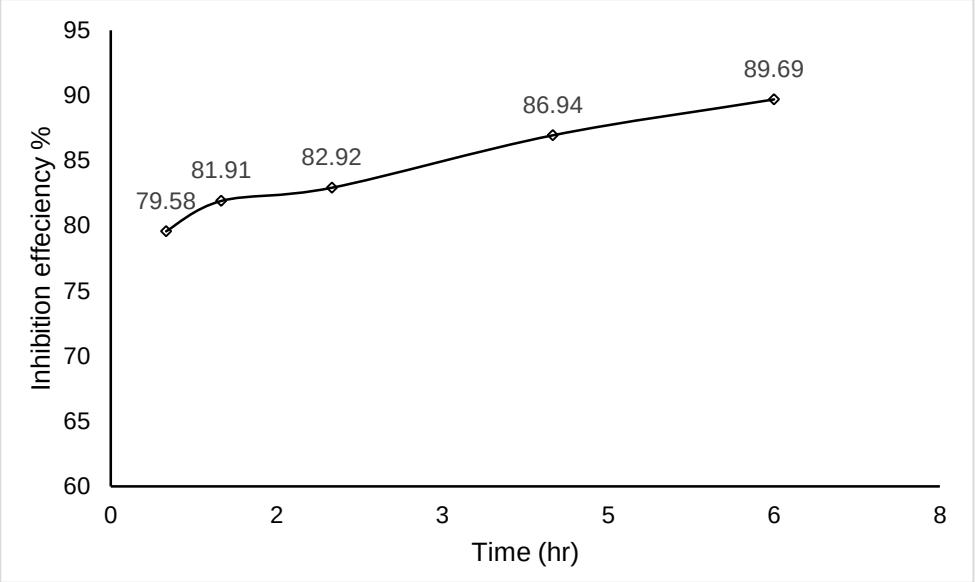

Figure 11. Variation of *IE* with immersion time of LCS in 0.5 M H_2SO_4 containing 8 mM cysteine + 25 µM Cu^{2+} ions.

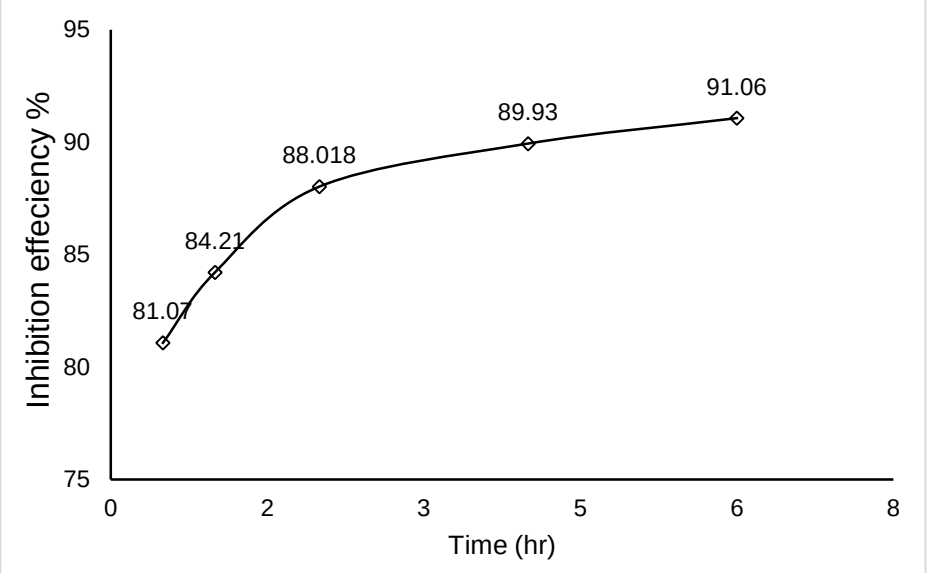

Figure 12. Variation of *IE* with immersion time of LCS in 3.5 wt% NaCl + 0.5 M H_2SO_4 containing 8 mM cysteine + 25 µM Cu^{2+} ions.

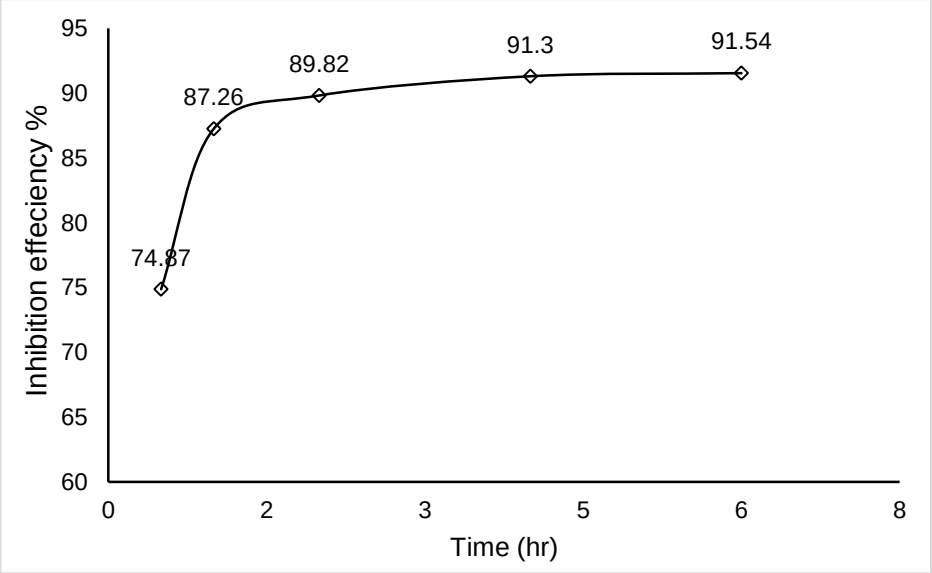

Figure 13. Variation of *IE* with immersion time of LCS in 0.5 M Na_2SO_4 + 0.5 M H_2SO_4 containing 8 mM cysteine + 25 µM Cu^{2+} ions.

3.5. Surface characterization

Scanning electron microscopy (SEM) was conducted to characterize inhibited sample surfaces and to evaluate the efficiency of inhibitor blend. The SEM results of the polished and corroded LCS samples are shown in Fig. 11. The figure shows the sample surface scan results after one day of immersion in the three testing solutions (A, B and C) in the absence and presence of inhibitor blend. Figure 14 (image a) represents the SEM image for polished LCS sample surface. While Figure 14 (images b and c) shows the SEM images of LCS surface in the uninhibited medium (A) and with inhibitor blend (8 mM cysteine + 25 µM Cu(II)). Figure 14 (images d-g) shows SEM images of LCS surface in media (B) and (C) without and with inhibitor blend, respectively.

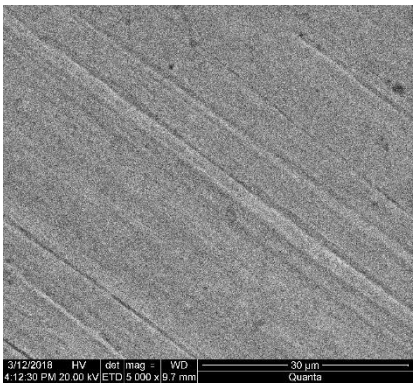

Figure 14.a SEM image for polished LCS sample surface

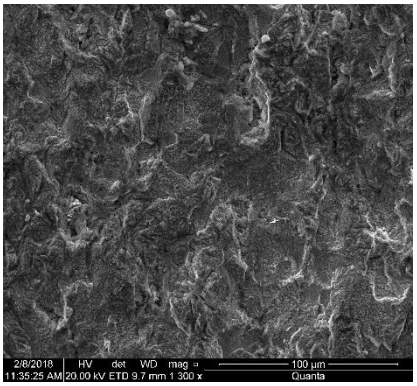

Fig.14.b LCS in medium A (0.5 M H_2SO_4)

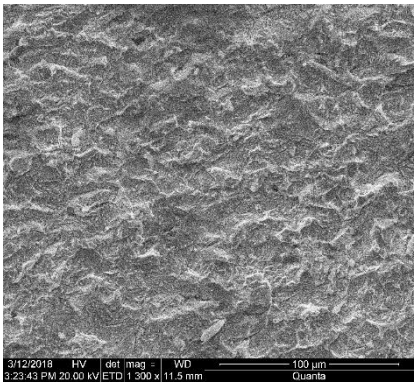

Fig.14 C. LCS in A + 8 mM cystiene+25µM Cu^{2+}

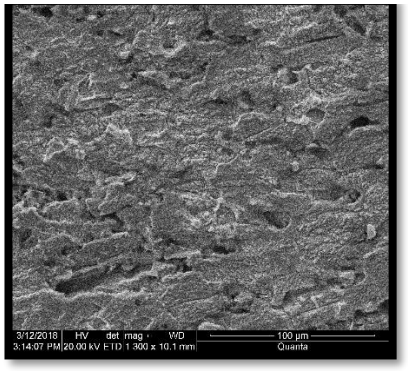

Fig.14.d LCS in medium B (3.5 wt% NaCl + 0.5 M H_2SO_4)

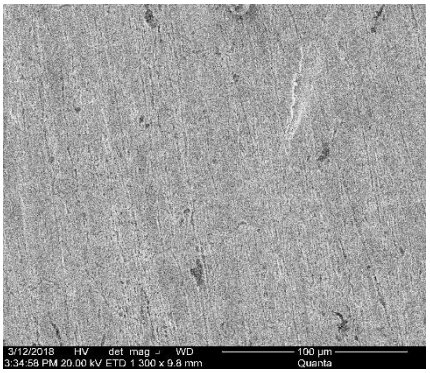

Fig.14.e LCS in B + (8 mM cystiene+25µM Cu^{2+})

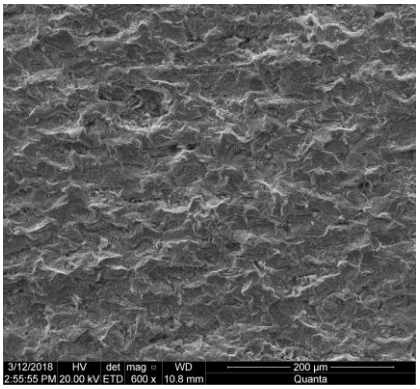

Fig.14.f LCS in medium C: (0.5 M Na_2SO_4 +0.5 M H_2SO_4)

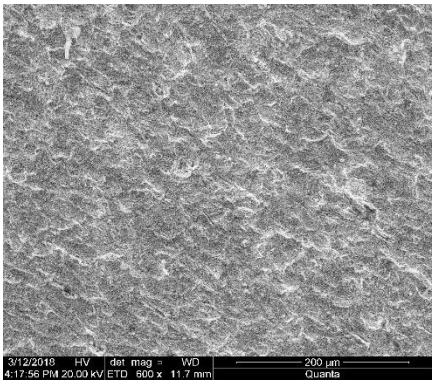

Fig.14.g LCS in C +(8 mM cystiene+25µM Cu^{2+})

Figure 14. SEM images.

The results demonstrate that in the absence of the inhibitor in the testing solutions, the surface corrosion are relatively clearly higher and sample surfaces are severely damaged(Fig. 14-b,d,f) compared to the sample surfaces immersed in the corrosive solutions with the presence of inhibitor blend(Fig. 14-c,e,g). These observations reveal that the inhibitor blend form a protection film on the LCS surface by adsorbed inhibitor molecules which prevents corrosive agents reaching the surface and thereby reducing the corrosion rate.

3.6. Corrosion inhibition mechanism and results of EDX

Presented results clearly show that cysteine- copper ions blend is an effective inhibitor of low carbon steel corrosion in the three testing corrosive media. The plots of potentiodynamic results in Fig. (8,9 and 10) prove that the inhibitor blend performs as a mixed-type inhibitor, reducing both partial (oxidation and reduction) corrosion reactions. The mechanism of its inhibition performance is by forming a surface protection layer, by the formation of Cu(I)–cysteinate complex [44-48] and/or cysteine (SAM) self-assembled monolayer at Cu atop LCS surface [49], which minimizes access of corrosive agents to the surface of low carbon steel due to the presence of a tight hydrophobic barrier. The inhibition efficiency depends on the surface coverage and then the concentration of adsorbed inhibitor molecules on the metal surface. In this regard to estimate the tight of the cysteine-copper ions blend inhibitor layer on the CS surface, EDX measurements were performed. EDX results shown in Table 11 indicate a significant increase in the weight percentage of carbon, oxygen, sulphur, nitrogen (which are the most element content of the inhibitor molecule) and copper elements on the surface of LCS sample immersed for 1 hour in the three corrosive media (A,B and C) in present of 8 mM cysteine and 25 µM Cu^{2+}. These increasing of element percentages on the sample surface of low carbon steel are proportional with quantity of adsorbed inhibitor on the surface and then with the metal surface coverage.

Table 11. EDX spectral data for the surface analysis of LCS subjected to the three media for 1 hour in the presence of inhibitor blend (8 mM of cysteine + 25 µM of Cu^{2+} ions).

Element on sample surface	Wt. % on LCS surface			
	Fresh sample	After immersing in inhibited solution for 1 hour		
		Medium A	Medium B	Medium C
Carbon	1.15	4.55	4.25	3.05
Oxygen	1.66	4.43	4.24	4.28
Nitrogen	0.122	0.68	0.96	0.68
sulphur	0.19	0.21	0.22	0.38
Copper	0.031	0.44	0.32	0.40

4. CONCLUSIONS

The following could be concluded:

1. The influence of the addition of Ni^{2+}, Fe^{2+} and Cu^{2+} ions (in micro-molar concentration range) for cysteine (as eco-friendly corrosion inhibitor for LCS) revealed that only Cu^{2+} ions have improved the corrosion inhibition efficiency (IE) of cysteine for LCS. IE values of cysteine against the corrosion of LCS in acidic solution is greatly improved in the presence of 25 μM Cu^{2+} ions, in chloride-containing acidic medium.

2. EIS, weight-loss and polarization measurements consistently revealed the high and good long-lasting effective corrosion inhibition efficiency of cysteine-Cu(II) ions blend for LCS in the three testing media (A, B and C) at low concentration of cysteine(8 mM).

3. Potentiodynamic measurements demonstrated that cysteine-copper ions blend acts as a mixed-type inhibitor reducing both cathodic as well as the anodic partial reactions.

4. The inhibition process of the cysteine-Cu(II) blend might originate from the formation of adher layer atop the surface of LCS thus minimizes access of solvated corrosive agents to LCS surface as evidence from EDX and SEM results.

References

1. X. Jiang, Y. G. Zheng, D.R. Qu, W. Ke, *Corros. Sci.,* 48 (2006) 3091.
2. W. Villamizar, M. Casales, J. G. Gonzalez-Rodriguez, L. Martinez, *J. Solid State Electrochem*., 11 (2007) 619.
3. S. Papavinasam, A. Doiron, T. Panneerselvam, R. W. Revie, *Corros.*, 63 (2007) 704.
4. S. Modiano, C.S. Fugivara, A.V. Benedetti, *Corros. Sci*., 46 (2004) 529.
5. M.A. Migahed, *Progress in Organic Coatings,* 54 (2005) 91.
6. M.A. Deyab, *Corros. Sci*., 49 (2007) 2315.
7. M. Knag, J. Sjoblom, *J. Dispers. Sci. Technol*., 27 (2006) 65.
8. M. Abdallah, E.A. Helal, A.S. Fouda, *Corros. Sci*., 48 (2006) 1639.
9. L. Smith, *British Corros. J.* 34 (1999) 247.
10. A.G. Petersen, D. Klenerman, W.M. Hedges, *Corros.*, 60 (2004) 187.
11. A. Turnbull, D. Coleman, A.J. Griffiths, P.E. Francis, L. Orkney, *Corros.,* 59 (2003) 250.
12. G. Gusmano, P. Labella, G. Montesperelli, A. Privitera, S. Tassinari, *Corros.,* 62 (2006) 576.
13. X. Zhang, F. Wang, Y. He, Y. Du, *Corros. Sci*., 43(2001) 1417.
14. M.B. Kermani, A. Morshed, *Corros.*, 59 (2003) 659.
15. M. M. El-Rabiee, N.H. Helal, G.M. Abd El-Hafez, W.A. Badawy, *J. Alloys Compd*., 459 (2008) 466.
16. M.S. Morad, *J. Appl. Electrochem*., 37 (2007) 1191.
17. M.S. Morad, *J. Appl. Electrochem*., 35 (2005) 889.
18. Y. Okazaki, E. Gotoh, *Biomater*., 26 (2005) 11.

19. E.E. Oguzie, Y. Li, F.H. Wang, *Electrochim. Acta,* 53 (2007) 909.
20. Yurt, A. Balaban, S.U. Kandemir, G. Bereket, B. Erk, *Mater. Chem. Phys.,* 85 (2004) 420.
21. W.P. Singh, J.O. Bockris, The NACE International Annual Conference and Expedition, paper no. 225, 1996.
22. W.M. Hedgaes, S.P. Lockledge, The NACE International Annual Conference and Expedition, paper no. 151, 1996.
23. M.A. Kiani, M.F. Mousavi, S. Ghasemi, M. Shamsipur, S.H. Kasemi, *Corros. Sci.,* 50 (2008) 1035.
24. K.M. Ismail, Electrochim. Acta, 52 (2007) 7811.
25. J.B. Matos, L.P. Pereira, S.M.L. Agostinho, O.E. Barcia, G.G.O. Cordeira, E. D'Elia, *J. Electroanal. Chem*., 570 (2004) 91.
26. D. Q. Zhang, H. Zeng, L. Zhang, P. Liu, L. X. Gao, *Colloids Surf. A: PhysicoChem. Eng. Aspects*, 445 (2014) 105.
27. D. A. Zhang, L.-X. Gao, G.-D. Zhou, *J. Appl. Electrochem*., 35 (2005) 1081.
28. E. B. Ituen, O. Akaranta, S. A. Umoren, *J. Mol. Liquids*, 46 (2017) 112.
29. M. Mobin, S. Zehra, M. Parveen, J. Mol. Liquids, 216 (2016) 598.
30. X. Zhou, Y. Xiao, X. Meng, B. Liu, Food Chem., 266 (2018) 1.
31. A.B. Silva, S.M.L. Agostinho, O.E. Barcia, G.G.O. Cordeiro, E. D'Elia, *Corros. Sci*., 48 (2006) 3668.
32. Ulman, An Introduction To Ultrathin Organic Films From Langmuir-Blodgett To Self-Assembly, Academic Press, London, 1991.
33. J.J. Gooding, F. Mearns, W. Yang, J. Liu, *Electroanal.*, 15 (2003) 81.
34. C.J. Zhong, J. Zak, M.D. Porter, *J. Electroanal. Chem*., 421 (1997) 9.
35. M.S. El-Deab, T. Ohsaka, *Electrochem. Commun*., 5 (2003) 214.
36. Hui Cang, Zhenghao Fei, Wenyan Shi, Qi Xu, *Int. J. Electrochem. Sci.,* (7)(2012) 10121.
37. Mohammad Mobin , Saman Zehra, Mosarrat Parveen, *J. Mol. Liq.,* 216 (2016) 598.
38. Mohamed S. El-Deab, Mater. Chem. Phys., 129 (2011) 223– 227.
39. Ghareba, S., S. Omanovic, *Electrochim. Acta*, 56(2011) 3890.
40. S.Y. Sayed, M.S. El-Deab, B.E. El-Anadouli, B.G. Ateya, *J. Phys. Chem*. B, 107 (2003) 5575.
41. ASTM G 31-72 Standard Practice for Laboratory Immersion Corrosion Testing of Metals (re-approved 1995), 03.02, 1990.
42. R. Martinez-Palou, J. Rivera, L.G. Zepeda, A.N. Rodriguez, M.A. Hernandez, J. Marin-Cruz, A. Estrada, *Corros.*, 60 (2004) 465.
43. G. Gao, C.H. Liang, H. Wang, *Corros. Sci.,* 49 (2007) 1833.
44. K.M. Ismail, *Electrochim. Acta,* 52 (2007) 7811.
45. J.B. Matos, L.P. Pereira, S.M.L. Agostinho, O.E. Barcia, G.G.O. Cordeira, E. D'Elia, *J. Electroanal. Chem.,* 570 (2004) 91.
46. C.M.G. van den Berg, B.C. Househam, J.P. Riley, *J. Electroanal. Chem*., 239 (1988) 137.
47. S. Cakir, E. Bicer, O. Cakir, Electrochem. *Commun.,* 2 (2000) 124.
48. I.M. Kolthoff, W. Stricks, *J. Am. Chem. Soc*., 73 (1951)1728.
49. S. Kuwabata, H. Kanemoto, D. Oyamatsu, H. Yoneyama, *Electrochemistry*, 67(1999) 1254.